14,15

Change of fractal geometry of microcracks during deformation: X-ray microtomography, acoustic emission and discrete element modeling

© E.E. Damaskinskaya[1], V.L. Hilarov[1], Yu.S. Krivonosov[2], A.V. Buzmakov[2], V.E. Asadchikov[2], D.I. Frolov[1]

[1] Ioffe Institute,
St. Petersburg, Russia
[2] National Research Centre „Kurchatov Institute“,
Moscow, Russia

E-mail: Kat.Dama@mail.ioffe.ru

Received June 4, 2024
Revised June 11, 2024
Accepted June 12, 2024

The aim of the work was to directly observe and further analyze defects (microcracks) developing in the sample volume of natural heterogeneous material under the action of uniaxial compressive load. X-ray computed microtomography was used to detect defects in the volume. The peculiarity of the experiments is that tomographic survey of the sample under the action of load was performed. Based on the analysis of tomographic data, three-dimensional models of the defect structure were constructed and the fractal dimension of the microcrack system was calculated. Numerical experiments on the fracture of samples of heterogeneous materials were carried out using the discrete element model. The change of fractal dimension of foci of destruction during their growth is investigated. A good agreement between the results of computer modeling and laboratory experiments has been established, which allows us to speak about the adequacy of the proposed model.

Keywords: X-ray micro-CT, defect evolution, computer modeling, discrete element method, acoustic emission, fractal dimension

DOI: 10.61011/PSS.2024.09.59230.144

1. Introduction

Destruction of natural heterogeneous materials due to occurrence and development of defect structure is a multistage process developing in time and space [1–8]. In order to separate thees stages and understand the physical reasons that control transition from one stage to another one, it is necessary to obtain information on evolution of the defect structure in volume of the deformed material. The experimental method ensuring visualization of three-dimensional internal microstructure of objects, i.e. to „view“ defects and determine their geometrical characteristics in volume of massive opaque sample, can be X-ray microtomography (X-ray micro-CT). The main advantage of this method is that the sample in this case keeps its integrity.

In papers [9–16] using X-ray micro-CT we study the microcracks formed as result of mechanical action. As a rule, tomographic measurements is made either after mechanical tests completion or after each stage of loading [9–12]. At that during tomographic experiment the sample is in unloaded state.

In [13–14] experiments are described, when tomographic studies of samples in loaded state were performed. The cracks system development was observed with load increasing. But cracks propagation was not quantitatively described.

Due to this the first objective of the paper is direct observation and analysis of morphology of system of microcracks developed in volume of sample of natural heterogeneous material (mine rock) under action of uniaxial compressive load.

The results, obtained using tomographic studies, can give only geometric characteristics of cracks. At same time, to identify the physical reasons of destruction development, we need presentations of local values of different mechanical parameters (deformation and stresses).

The second objective of the paper means the features of development of main crack (foci of destruction) in computer model of destruction based on the Discrete Element method comparison with experimental data. In case of satisfactory agreement of the results, this computer model is tool to study local parameters, which currently can not be measured (determined) by experimental methods.

2. Experiment

Berea sandstone [17] was chosen as the material for the research, it is standard material for experiments on deformation of rock samples. Mineral composition of Berea sandstone is shown in Table 1. The Berea sandstone mainly comprises quartz grains with characteristic size $20\,\mu$m. Samples have cylindrical shape ($d = 10$ mm, $h = 20$ mm). Sample end faces were additionally polished to ensure their

Table 1. Mineral composition of Berea sandstone

Mineral	Quartz (quartz)	Plagioglase (plagioclase)	K-feldspar (feldspar)	Kaolinite (Kaolinite) (aluminum silicate)	Calcite (Calcite) $CaCO_3$
	85–90%	1–2%	3–6%	2–6%	6–8%
Density	2600–2650 kg/m^3	2620–2760 kg/m^3	2560 kg/m^3	2600 kg/m^3	2710 kg/m^3

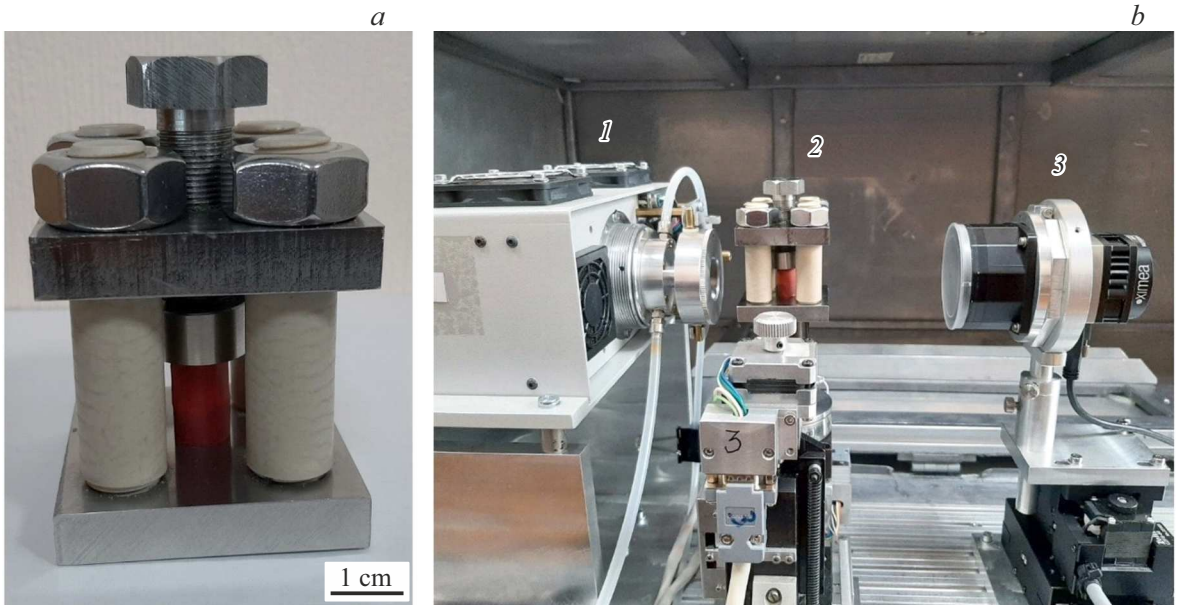

Figure 1. Experimental set-up: *a* — photo of loading cell with sample installed; *b* — optical part of X-ray microtomograph „MICROTOM“: *1* — source, *2* — loading cell with sample, *3* — detector.

flatness. Side surface of samples before experiments was fixed using heat shrink material to prevent spillage during deformation.

The experiments feature was that micro-CT of sample under load was performed. For this purpose special portable loading cell (see Figure 1, *a*) was developed, from one hand it ensures required load, and, on other hand, was placed into tomograph chamber and did not prevent measurements. Four support posts of the loading cell were made as cylinders with diameter of 16 mm of polyesteresterketon (PEEK), which has required strength and low absorption coefficient in hard X-ray range. This made it possible to view the sample under conditions where the sample itself was in the detector's field of view, and the PEEK support posts were not in the detector's field of view over a significant portion of the projections. During preliminary experiments the tomography results of sample without the cell and with it were compared, this confirmed possibility of use the suggested experiment conditions.

Tomographic measurements were performed on a cone-beam X-ray microtomograph „MICROTOM“, developed and created at the National Research Centre „Kurchatov Institute“ [18]. Image of the optical part of microtomograph with installed loading cell and sample is given in Figure 1, *b*. In tomograph a microfocus polychromatic X-ray source with molybdenum transmission target and focal spot size 15–20 μm is used. For the experiment accelerating voltage 80 kV was selected. The tomographic projections of sample measured at different angles were registered by X-ray detector XIMEA with matrix 2968×5056 elements and pixel size 8.5 μm. The experiments were performed in the following geometry: distance source — sample 50 mm and source — detector 150 mm, geometric zoom $M = 3.0$. In each experiment 720 projections were registered in range of angles 360 degrees. 3D images of objects were restored using FDK algorithm [19]. To reduce the „cupping effect“, which is artifact and occurs due to the „hardening“ of the polychromatic beam when passing through the sample, Al — filter with thickness 0.36 mm was installed between the source and the sample. Besides, for complete removal of the cupping-like artifact the procedure of automatic gamma — correction, described in paper [20], was applied to initial normalized and logarithmic sinograms. Also note that considering the suggested geometry of the experiment the sample tomography was made not for the entire sample, but for its central part with height 7 mm.

Before tests commencement the tomographic study of the complete party of sandstone samples was performed.

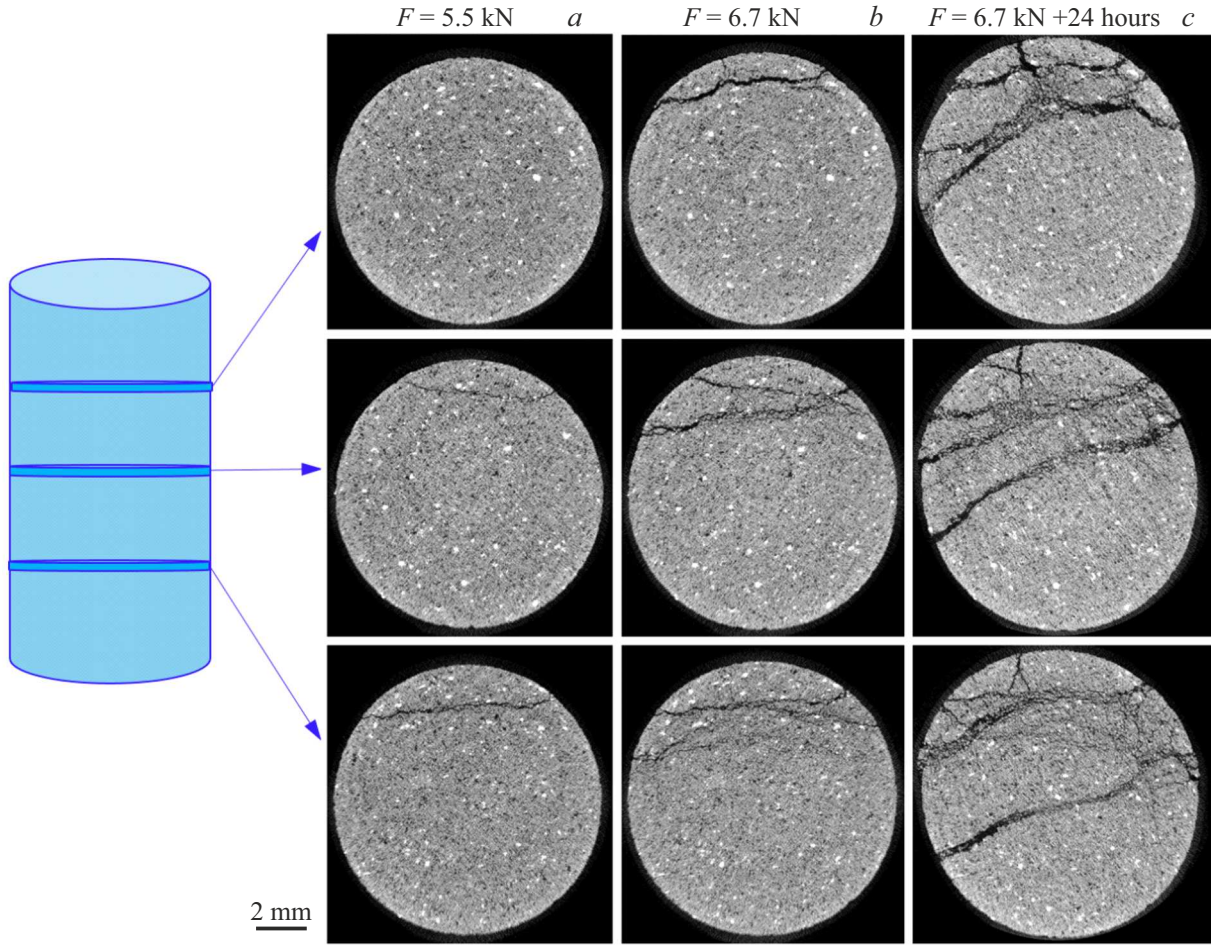

Figure 2. Distribution o X-ray optical density in sample sections located in its top, central and bottom portions, after first (a), second (b) and third (c) stages of loading.

For further experiments we selected samples which do not contain structural anomalies that can be stress concentrators and sources of defects occurrence and destruction development.

The experiment was performed in several stages. At the first stage the sample was subjected to compression in cell up to load 5.5 kN. The cell was installed in the tomograph and micro-CT was performed. At second stage the load was increased to 6.7 kN, and measurement was repeated. Then sample was held for 24 h under load. Further, sample lost stability when attempt to increase the load was made. After that final micro-CT was made.

Note that during the entire experiment the sample was all time under load.

3. Results and discussion

3.1. Laboratory experiment

During these experiments the contrast is associated with X-rays absorption during passage through the object of study. As the sample material is heterogeneous, the absorption coefficients of different components differ. As a result, after tomographic reconstruction we obtain pictures of X-ray optical density distribution in different horizontal sections of the sample. Figure 2 shows sample sections through height obtained at three stages of loading. The grayscale values correspond to different X-ray optical densities of the material. Black lines — cracks. We see that after first loading the crack does not pass through the entire sample (Figure 2, a). Load increasing results in crack propagation (Figure 2, b). Holding for a day under load 6.7 kN resulted in loss of sample stability. We clearly see that crack became more developed (Figure 2, c).

To segment cracks formed in sample during stage-by-stage loading thresholding of tomographs using global threshold was performed. After thresholding multiple isolated pores initialy present un the sample and not associated with the formed cracks were removed. Similarly the fragments of sample material were from the binary image, if they were isolated in volume of cracks, and were not associated with massive of sample. This procedure was performed using utility of unbound voxels search in program package Python Toolkit „Porespy“ [21]. Figure 3, $a-c$ shows

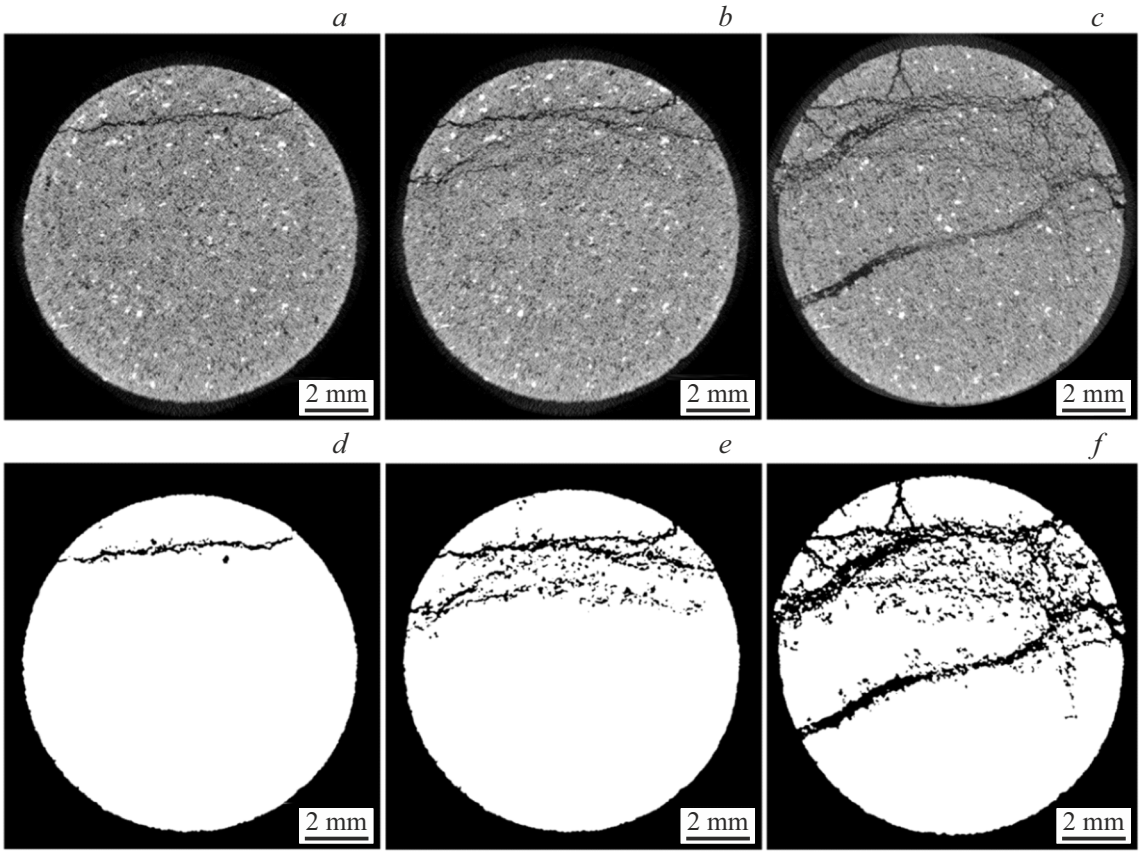

Figure 3. Tomographic sections of sample in grayscale (top) and corresponding binary images (bottom) after each loading stage: (*a*), (*d*) — 1-st stage; (*b*), (*e*) — 2-nd stage; (*c*), (*f*) — 3-rd stage.

the tomographic sections of sample made at the same height in bottom portion of sample after each loading stage, and appropriate final binary images (Figure 3, *d–f*), being basis for further calculation of crack parameters.

To further morphology analysis of the crack system we used fractal theory. In papers [11,12,15,16] the fractal dimension of cracks or pores was calculated. It was shown that fractal dimension is sensitive to degree of heterogeneity of the material due to its stressed state. In this paper the fractal dimension calculated by box counting method (BCM) [12,22,23] was selected as quantitative characteristic of the defect structure. Substantially, this is the dimension D_0 from set of Renyi fractal dimensions [24]. Using this method we calculated the fractal dimension of surfaces of cracks based of three-dimension models of crack reconstruction.

It is identified that after 1 loading stage (at load 5.5 kN) the fractal dimension of crack is 1.8. This means that the crack is openwork and with dimension close to a plane. Load increasing to 6.7 kN results in crack development — fractal dimension increases to 2.3. At third stage of deformation value of the fractal dimension reaches 2.6. Actually, we can see that shape of the crack becomes more branched and occupies practically the entire volume of sample. This is clearly illustrated by the tree-dimensional visualization of the microcracks system made as per results of tomography (Figure 4).

3.2. Computer modeling

To determine the relationship of processes occuring at the microlevel with the macroscopic realizations, as well as local parameters that cannot be measured experimentally, a computer model of the destruction of heterogeneous material was previously constructed. The model is based on the discrete element method (DEM), and is described in detail in [25,26]. In our paper we used the bonded particle model [27] (BPM), which helps to study the the evolution of defects in detail. Calculations using the discrete element method (DEM) were performed in the freely distributable software package MUSEN [28]. Material (rock) model contains spherical particles of the same or different sizes simulating the grains and particle bonds simulating the grain boundaries.

BPM defines cracking nucleation as bond breaking between particles and their propagation — as merging of a multitude of broken bonds. To get a crack from a set of bonds broken from the beginning of the experiment up to a particular time moment, a clustering procedure

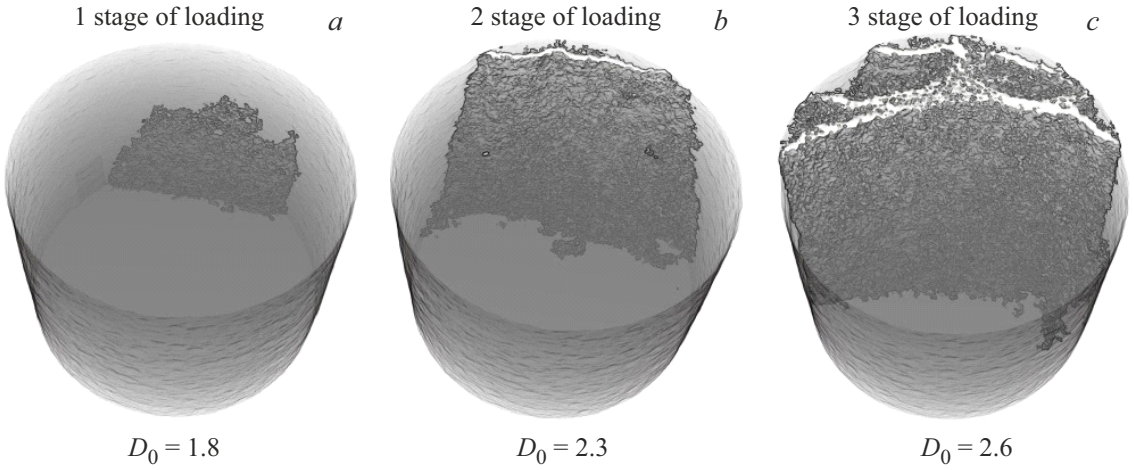

Figure 4. Three-dimension visualization of crack after three loading stages. Dark-gray objects of complex geometric shape inside the sample — formed cracks.

Table 2. Grain diameters (mm) and percentage composition of each of the fractions

	Grain diameter of different fractions d_i, mm					Portion of each fraction
Quartz	0.09	0.047	0.132	0.079	0.106	0.0595745
Orthoclase	0.068	0.07	0.096	0.91	0.064	0.0702128
Oligoclase	0.041	0.042	0.077	0.063	0.098	0.0702127

Table 3. Parameters of materials used for simulation

№	material	ρ, kg/m^3	E, GPa	ν	σ_n, MPa	σ_t, MPa	η, Pa · s
1	quartz	2650	94	0.29	600	600	5E19
2	orthoclase	2560	62	0.29	420	420	1E19
3	oligoclase	2560	70	0.29	480	480	1E19

Note. ρ — material density, E — Young's modulus, ν — Poison's ratio, σ_n — tensile strength of material, σ_t — shear strength of material, η — dynamic viscosity.

(merging of broken bonds according to the selected algorithm, which will be described below) is required. Thus, defects are hereinafter referred to as the broken bond clusters.

The computer experiment scheme is similar to that described in [26]. Cylindrical samples of the diameter 10 mm and height 20 mm were modelled. The sample was placed into a virtual press. The lower plate was fixed, and the upper plate moved downwards at a constant speed. Thus, uniaxial compression was simulated. The experiment was finished with failure of the sample (separation into parts). During the experiment, a large set of various mechanical parameters was recorded in equal time periods — data storage interval — to be further used for analysis. This time interval was chosen according to the process stationarity conditions. Positions of the centers of bonds broken during the sample deformation and bond breaking times were such parameters herein.

Numerical experiments with samples having different structure were performed. Material and size of particles, material and diameter of bonds were varied. In all cases we succeeded to determine general patterns of the fractal properties of the foci of destruction (main cracks) [29]. In present paper these results are provided as example for one type of samples.

Sample contains the particles with diameters and percentage composition as listed in Table 2 (the number of particles is 33670). This is a set of sizes with a mean value of 0.08 mm and a standard deviation of 0.025 mm which was obtained by random number generator with normal distribution (Table 2). Fraction 4 diameter for orthoclase is increased by an order of magnitude to improve the degree of heterogeneity. There were only orthoclase bonds with a diameter of 0.04 mm. Physical and mechanical parameters of the materials that constitute the particles and bonds are listed in Table 3.

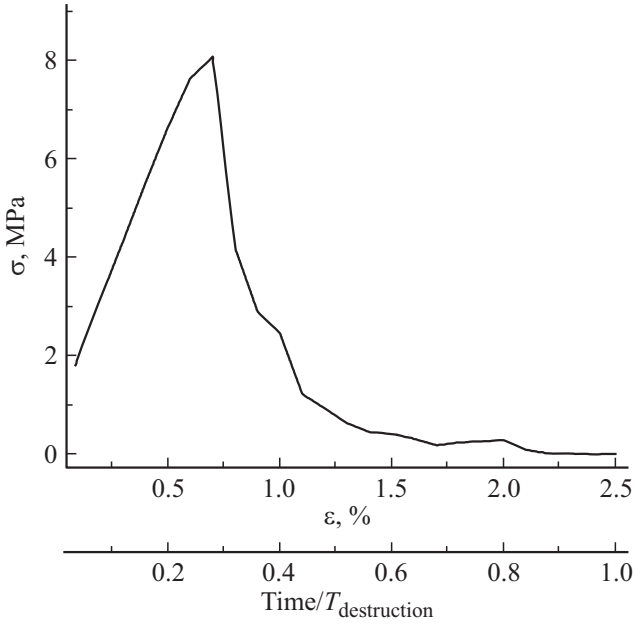

Figure 5. Stress change on sample during computer experiment. Second horizontal axis corresponds to standardized experimental time ($T_{destruction}$ — time moment when sample was divided into parts).

Figure 5 shows change of stress during experiment. It is obvious that this sample brittle destructed, this is natural to sandstone.

To study the defects evolution the broken bond clustering was performed. The DBSCAN (density-based spatial clustering of applications with noise [30]) algorithm was used for clustering on the basis of the density of cluster components.

Clustering of bonds broken from the beginning of loading until time t_k provides the picture of defects (cracks) which formed by this time moment (t_k). For this, the defect size is assumed equal to the number of bonds combined into this cluster.

In computer experiments, like in laboratory one, we studied fractal properties of the foci of destruction. The fractal dimension was calculated based on spatial location of bonds forming the center at the different time moments.

The correlation fractal dimension D_2, calculated based on Grassberger and Procaccia correlation function [31] (correlation integral) is considered as the main characteristic:

$$C(r) = \frac{2}{N(N-1)} \sum_{j=1}^{N} \sum_{i=j+1}^{N} H(r - r_{ij}) \qquad (1)$$

Here r_{ij} is the distance between pair of broken bonds, (between the coordinates of their centers), N — number of analyzed broken bonds, H — Heaviside function equal to 1 if its argument is positive, otherwise equal to 0. So, function (1) is equal to number of pairs of events, distance between which does not exceed r. If the considered system has scale invariance, the dependence $C(r) \propto r^d$, i.e. it is a power function with an exponent equal to fractal dimension of set. Dimension d in this case is called the correlation fractal dimension. In is shown in [31,32] that this value is equal to dimension D_2 from set of Renyi fractal dimensions [32].

Change of fractal dimension of the foci of destruction (maximum cluster) was analyzed. Figure 6 shows development of the foci of destruction at successive time moments. In Figure 7 the graph of change of fractal dimension of this foci during experiment is plotted. Initially the foci is approximately flat with fractal dimension ($D_2 \sim 2$). Its growth results in that destruction covers ever increasing volume, this is accompanied by increase in fractal dimension.

Note that same behavior of the correlation fractal dimension (D_2) during foci of destruction development was observed earlier when analyzing data of acoustic emission registered during laboratory experiment [33].

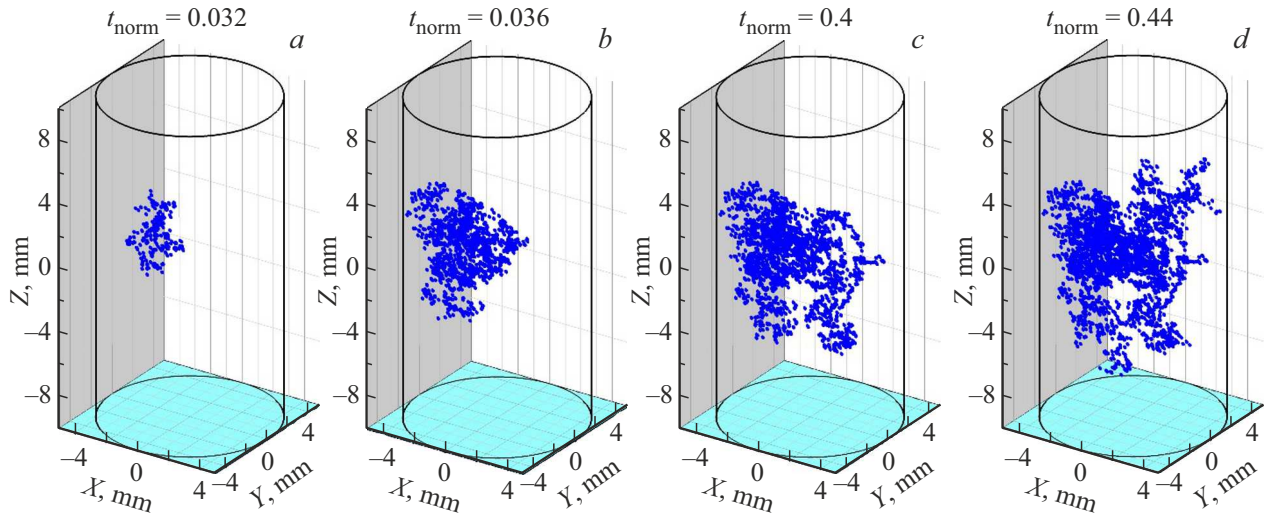

Figure 6. Development (propagation of foci of destruction in computer experiment. Here t_{norm} = Time/$T_{destruction}$, (i.e. normalized time).

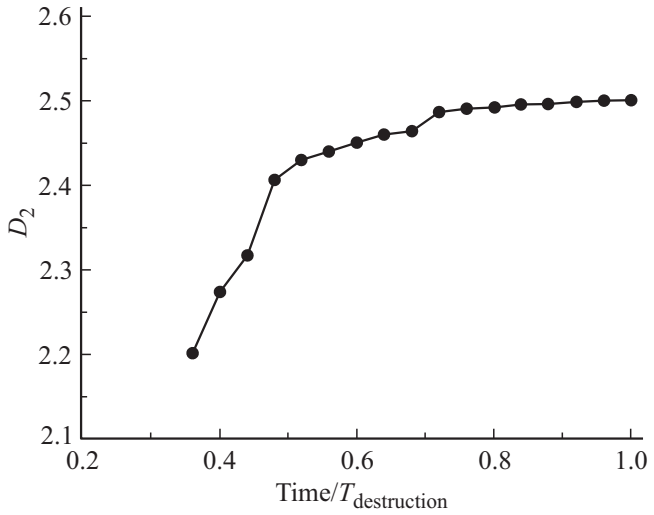

Figure 7. Change in fractal dimension of foci of destruction in computer experiment.

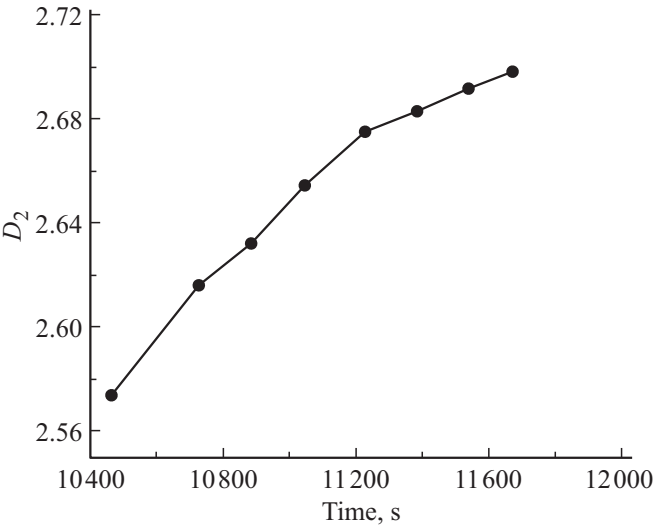

Figure 8. Dependence of correlation fractal dimension of coordinates of hypocenters of acoustic emission signals in laboratory experiment.

In these experiments, see details in [1], cylindrical samples of Westerly granite ($h = 190.5\,\text{mm}$, $d = 76.2\,\text{mm}$) were loaded. Samples were deformed under constant pressure and uniaxial axial loading. Monitoring of the cracking was ensured by signals registration of acoustic emission (AE). Unlike previous papers [34], where the fractal dimension of sequences of sources of signals emitted during successive time intervals (or sequences of a given number of signals), in present paper we consider the increasing time intervals starting at same time point. This point corresponds to start of localized destruction (growth of predominantly one crack). Figure 8 shows change of the correlation fractal dimension of coordinates of hypocenters of acoustic emission signals registered from region of foci of destruction (main crack). It is obvious that in this experiment the fractal dimension of the foci increases, i.e. the main crack becomes branched, and gradually covers the ever greater volume.

4. Conclusion

Fractal geometry evolution of microcracks in the natural heterogenous material is studied in this paper. Direct monitoring of defects in sample under load is performed by X-ray computer microtomography. Based on analysis of the tomographic sections the fractal dimension is calculated for microcracks system, and three-dimension models of defect structure are constructed. It is shown that fractal dimension increases with load increasing. This clearly shows how the microcracks system becomes more developed and gradually occupies an ever larger volume.

Using computer model of destruction of heterogeneous material, based on the discrete element method, the formation and development of defects during loading is studied. The computer experiments ensure determination of details of fractal structures formation of foci of destruction. We suppose that this model can be considered as a tool to study the effect of local factors (heterogeneity of grains and their boundaries by size and mechanical properties, deformation etc.) on the macroscopic behaviour of loaded mine rock.

The obtained results also well agree with the results of laboratory experiments on study the acoustic emission during destruction of heterogeneous materials under mechanical load.

Funding

This study was carried out under the State Assignment of Ioffe Institute in terms of problem setting, analysis of results, computer modeling and processing of experiments using the acoustic emission method. This study was carried out under the State Assignment of NRC „Kurchatov Institute“ in relation of execution and processing of tomographic experiments.

Conflict of interest

The authors declare that they have no conflict of interest.

References

[1] D.A. Lockner, J.D. Byerlee, V. Kuksenko, A. Ponomarev, A. Sidorin. Nature **350**, 39 (1991).
[2] L.R. Botvina. Fizika Zemli, **10**, 5 (2011). (in Russian).
[3] M. Petružálek, J. Vilhelm, V. Rudajev, T. Lokajíček, T. Svitek. Int. J. Rock Mech. Mining Sci. **60**, 208 (2013).
[4] Y. Hamie, O. Katz, V. Lyakhovsky, Z. Reches, Yu. Fialko. Geophys. J. Int. **167**, 1005 (2006).
[5] V. Kuksenko, N. Tomilin, E. Damaskinskaya, D. Lockner. Pure Appl. Geophys, **146**, *2*, 253 (1996).
[6] V.B. Smirnov, A.V. Ponomarev, P. Bernar, A.V. Patonin. Fizika Zemli, **2**, 17 (2010). (in Russian).

[7] Xinglin Lei, Shengli Ma. Earthq. Sci. **27**, *6*, 627 (2014).
[8] Y. Tal, T. Goebel, J.P. Avouac. Earth and Planetary Sci. Lett. **536** (2020).
[9] Sheng-Qi Yang, P.G. Ranjith, Yi-Lin Gui. Geotech. Test. J., **38**, *2*, 179 (2015).
[10] S. Zabler, A. Rack, I. Manke, K. Thermann, J. Tiedemann, N. Harthill, H. Riesemeier. J. of Struct. Geology. **30**, 876 (2008).
[11] Yujun Zuo, Zhibin Hao, Hao Liu, Chao Pan, Jianyun Lin, Zehua Zhu, Wenjibin Sun, Ziqi Liu. Arabian J. of Geosciences. **15**, 1673 (2022).
[12] Yongming Yang, Yang Ju, Fengxia Li, Feng Gao, Huafei Sun. J. of Natural Gas Sci. and Engin. **32**, 415 (2016).
[13] X.P. Zhou, Y.X. Zhang, Q.L. Ha. Theor. and Appl. Fract. Mechanics. **50**, 49 (2008).
[14] J.X. Re. Soil and Rock Behavior and Modeling. https://doi.org/10.1061/40862(194)34
[15] Peng RuiDong, Yang YanCong, Ju Yang, Mao LingTao, Yang YongMing. Chinese Sci Bull. **56**, 3346 (2011).
[16] P. Liu, Y. Ju, F. Gao, P.G. Ranjith, Q. Zhang. J. Geophys. Res.: Solid Earth. **123**, 2156 (2018).
[17] P. Churcher, P. French, J. Shaw. SPE Intern. Symp. on Oilfield Chem. SPE21044 (1991).
[18] Yu.S. Krivonosov, A.V. Buzmakov, M.Yu. Grigoriev, A.A. Rusakov, Yu.M. Dymshits, V.E. Asadchikov. Kristallografiya, **68**, *1*, 160 (2023). (in Russian).
[19] Lee A., Feldkamp, Lloyd C. Davis, James W. Kress. JOSA. A. **1**, *6*, 612–619 (1984).
[20] A.S. Ingacheva, M.V. Chukalina. Math. Probl. in Engin. Article ID 1405365 (2019).
[21] J.T. Gostick, Z.A. Khan, T.G. Tranter, M.D. Kok, M. Agnaou, M. Sadeghi, Jervis, R. PoreSpy. J. of Open Source Software. **4**, 1296 (2019).
[22] Y. Ju, J.T. Zheng, M. Epstein, L. Sudak, J.B. Wang, X. Zhao. Comput. Methods Appl. Mech. Eng. **279**, *7*, 212 (2014).
[23] H.P. Xie. Fractals in Rock Mechanics. CRC PRESS, Boca Raton (1993). 464 p.
[24] R.D. Peng, Y.C. Yang, Y. Ju, Ju. Yang, Mao LingTao, Ming Yang. Chinese Sci. Bull. **56**, 3346 (2011).
[25] S.V. Bozhokin, D.A. Parshin. Fraktaly i mul'tifraktaly. NITs „Regulyarnaya i khaoticheslaya dinamika", Izhevsk. (2001). 128 s. (in Russian).
[26] V.L. Gilyarov, E.E. Damaskinskaya. FTT **64**, *6*, 676 (2022). (in Russian).
[27] D.O. Potyondy, P.A. Cundall. Int. J. Rock Mech. Min. Sci **41**, 1329 (2004).
[28] Dosta, V. Skorych. SoftwareX **12**, 100618 (2020).
[29] V.L. Hilarov, E.E. Damaskinskaya. Materialwiss. Werkstofftech. **54**, 1554 (2023).
[30] M. Ester, H.-P. Kriegel, J. Sander, X. Xu. In: Proc. of the Second Intern. Conf. on Knowledge Discovery and Data Mining (KDD-96) / Evangelos Simoudis, Jiawei Han, Usama M. Fayyad. AAAI Press, **226** (1996).
[31] P. Grassberger, I. Procaccia. Phys. Rev. Lett. **50**, 346 (1983).
[32] G. Shuster. Malomerny khaos. Mir, M. (1988). 240 s. (in Russian).
[33] T.C. Halsey, M.H. Jensen, L.P. Kadanoff, I. Procaccia, B.I. Shairman. Phys. Rev., B. **33**, *2*, 1141 (1986).
[34] V.L. Hilarov. Modeling Simul. Mater. Sci. Eng., **6**, 337 (1998).

Translated by I.Mazurov